Monte Carlo Simulations of Diblock Copolymer Thin Films Confined between Chemically Heterogeneous Hard Surfaces

Qiang Wang, Qiliang Yan, Paul F. Nealey, and Juan J. de Pablo*

Department of Chemical Engineering, University of Wisconsin−Madison, Madison, Wisconsin 53706-1691

Received August 3, 1999; Revised Manuscript Received February 22, 2000

ABSTRACT: Thin films of symmetric diblock copolymers confined between two hard, flat and parallel surfaces have been investigated by means of Monte Carlo simulations on a simple cubic lattice. The upper surface is homogeneous, either neutral or preferential to one of the two blocks, and the lower surface is stripe-patterned, with all the stripes having the same width $L_s/2$ and alternatively preferring A and B blocks with the same strength of preference. We studied the effects of surface configuration (including surface type, surface pattern period, and surface separation) on the morphology of confined diblock copolymer thin films. Our results show that two conditions are essential for obtaining macroscopically ordered (over micrometers) perpendicular lamellae in the confined films (with film thickness no less than the bulk lamellar period L_0): a stripe-patterned substrate with pattern period L_s comparable to L_0, which directs the ordering of perpendicular lamellae over a macroscopic scale, and a neutral or weakly preferential hard surface on the top of the confined films, which stabilizes the perpendicular lamellae. When the perpendicular lamellae complying with the lower surface pattern form throughout the entire film, undulations of the A−B interfaces in the perpendicular lamellae are observed if the upper surface is not truly neutral, which could have adverse effects for nanolithography.

Introduction

The microscopic or mesoscopic phase separation of diblock copolymers has attracted significant interest because of their potential applications in nanofabrication. In some applications, e.g., nanolithography, macroscopically ordered (over micrometers) lamellar structures perpendicular to a substrate are desirable. Such structures can be obtained by using thin films of symmetric diblock copolymers, which spontaneously self-assembly into lamellae at temperatures below the order−disorder transition (ODT). Perpendicular lamellae have been observed experimentally in thin films of symmetric diblock copolymer confined between two homogeneous surfaces when the surface preference is weak or neutral; transmission electron microscopy (TEM) or field emission scanning electron microscopy (FESEM) images show that the orientation of such lamellae is short-ranged (over tens to hundreds of nanometers).[1−3] On the other hand, recent experiments[4] and theoretical calculations[5−12] suggest that macroscopically ordered perpendicular lamellae can be obtained by depositing symmetric diblock copolymers on a stripe-patterned chemically heterogeneous surface where the surface pattern period L_s is comparable to the bulk lamellar period L_0.

The purpose of this work is to study the morphology that arises when thin films of symmetric diblock copolymers are deposited on chemically heterogeneous surfaces. In the following discussion, such surfaces are patterned with stripes of uniform width $L_s/2$ that alternatively prefer A and B blocks of the copolymer.

By casting symmetric diblock copolymers on stripe-patterned chemically heterogeneous substrates, Rockford et al. found that perpendicular lamellae can be directed by the underlying stripes on the substrates when the bulk lamellar period L_0 is commensurate with the surface pattern period.[4] Furthermore, the ordering of the perpendicular lamellae appeared to be long-range (over micrometers). Note that in their experiments, the film thickness for all samples was on the order of 30 nm, which is less than L_0, and the upper surface was exposed to air (free surface).[4]

Halperin et al. presented scaling arguments to discuss the effect of the surface pattern period L_s on the adsorption of symmetric $(AB)_n$ multiblock, linear copolymers from solution onto stripe-patterned surfaces.[5] These authors came up with simple but highly approximate criteria for the range over which self-similar layers associated with uniform adsorption can occur.[5]

Chen and Chakrabarti used a Cahn−Hilliard formalism to study the morphology of symmetric diblock copolymer thin films confined between two hard surfaces separated by a distance D.[6,7] The upper surface was neutral and the lower surface was stripe-patterned. These authors found various structures depending on L_s/L_0 and D/L_0.[6,7] However, their Cahn−Hilliard formalism is a relatively coarse-grained model. Their free energy expansion was obtained by using a local approximation for the higher order couplings, and their results may not be quantitatively correct in the strong segregation regime.[7]

Using a simple mean-field free energy approximation, Petera and Muthukumar studied the structure of symmetric diblock copolymer melts close to a patterned surface near the ODT.[8] Their results below the ODT showed that if L_s is very much larger than L_0, checkerboard morphology (defined later) is expected close to the surface. Only when the pattern period and the bulk lamellar period are comparable can perpendicular lamellae complying with the surface pattern be expected.[8]

Subsequently, Petera and Muthukumar employed a more refined two-dimensional self-consistent field theory to study the possible equilibrium structures of symmetric diblock copolymer thin films confined between two hard surfaces separated by a distance D; the upper surface was homogeneous and the lower surface was

10.1021/ma991293n CCC: $19.00
Published on Web 05/17/2000

stripe-patterned.[9] They lowered the temperature gradually across the ODT from a disordered state. Note, however, that different grid resolutions and tolerance in their numerical calculations changed the resultant morphology in some cases; this raises the possibility that their calculations did not always result in a global free energy minimum.[9]

More recently, Pereira and Williams applied a phenomenological model valid in the strong segregation limit to study the morphology of symmetric diblock copolymer thin films confined between a lower stripe-patterned and an upper neutral hard surface, where these authors only considered perpendicular lamellae of different periods forming throughout the entire film.[10,11] Subsequently, they extended the upper neutral surface to a homogeneous (preferential) hard surface, and took into account parallel lamellae and the mixed morphology of parallel lamellae near the upper homogeneous surface and perpendicular lamellae near the lower patterned surface.[12] However, such a phenomenological model does not take molecular details into account.[13] Furthermore, some types of morphology in confined films observed in this work were not considered; such prior knowledge of the possible morphology is crucial for applying the phenomenological model to the systems of interest.[13]

Despite the recent interest in diblock copolymers on stripe-patterned surfaces, simulations of such systems have not been carried out before. The results of simulations could complement and validate theoretical predictions and could resolve some of the discrepancies in the literature. More importantly, they could provide useful insights regarding molecular configurations in such systems that could serve to guide future experimental work.

In this paper, we present results from Monte Carlo simulations of the morphology of symmetric diblock copolymer thin films confined between two hard, flat and parallel surfaces. The upper surface is homogeneous, either neutral or preferential to one of the two blocks, and the lower surface is stripe-patterned. We study the effects of surface configuration (including surface type, surface pattern period, and surface separation) on the morphology of confined diblock copolymer thin films, and compare our results with earlier work in this area.

2. Model

2.1. Simple Cubic Lattice Model. The model employed in this work is the same as that employed in ref 14. Many of the details can be found in that reference; only a brief account is provided here. A symmetric diblock copolymer chain consists of the same number of A and B segments connected by bonds whose length is taken to be the lattice unit. Each segment occupies one lattice site, and each lattice site is occupied by at most one segment. A rectangular simulation box of dimensions L_x, L_y, and L_z is employed. Periodic boundary conditions (PBC) are imposed in the x and y directions. As shown in Figure 1, two flat surfaces are introduced through the lattice sites at $z = 0$ and $z = L_z + 1$, respectively. To represent hard surfaces, these lattice sites are not allowed to be occupied by polymer segments. Diblock copolymers are therefore confined to a thin-film geometry of thickness $D = L_z - 1$.

In our model, we only consider repulsion between nearest-neighbor A−B pairs separated by one lattice unit ($\epsilon_{A-B} > 0$), and we set $\epsilon_{A-A} = \epsilon_{B-B} = 0$. Interactions between vacancies (unoccupied lattice sites) and polymer segments are also set to zero. The chemically heterogeneous surfaces considered in this paper are patterned with stripes parallel to the x axis, as shown in Figure 1. The stripes consist of alternating sA (light regions) and sB (dark regions) sites, whose nature depends on the surface−block interactions. For simplicity, we set $\epsilon_{sA-A} = \epsilon_{sB-B} = 0$, and $\epsilon_{sA-B} = \epsilon_{sB-A} = 2\epsilon_{A-B}$ (which represents strong surface-block interactions[14]). The difference between ϵ_{sA-A} and ϵ_{sA-B} (ϵ_{sB-A} and ϵ_{sB-B}) can be viewed as a chemical potential difference between the two species at the sA (sB) regions. All the stripes have the same width $L_s/2$, where L_s is the period of the surface pattern. The upper homogeneous surface consists of sH sites; we set $\epsilon_{sH-A} = 0$ and $\epsilon_{sH-B} = \alpha_H\epsilon_{A-B}$, where $\alpha_H \geq 0$. Therefore, when $\alpha_H = 0$, the upper surface is a neutral surface, with no preference for either of the two blocks; when $\alpha_H > 0$, the upper surface repels B blocks, and is therefore preferential to A blocks (referred to as the "preferential surface").

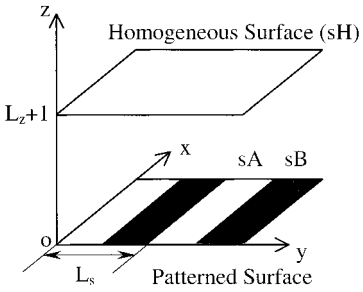

Figure 1. Configuration of the patterned-homogeneous surfaces. Both surfaces are hard and flat. The stripes on the lower patterned surface have the same width $L_s/2$ and alternatively prefer A and B blocks of the copolymer (denoted by sA and sB stripes, respectively). The upper homogeneous surface is either neutral or preferential to one of the two blocks.

2.2. Simulations in an Expanded Grand-Canonical Ensemble. We perform Monte Carlo simulations in a variant of the expanded grand-canonical ensemble method proposed by Escobedo and de Pablo.[15] The chemical potential and temperature of the simulated system are specified prior to a simulation. The confined copolymers are therefore in equilibrium with a bulk phase having the same chemical potential and temperature, and the density of the system is allowed to fluctuate during the simulation. In addition to molecule displacements by reptation moves and local (crankshaft and kink-jump) moves, we employ growing/shrinking moves performed four segments at a time to gradually insert/remove particles from the system. To facilitate transitions, configurational bias is used for these growing/shrinking moves, leading to an acceptance rate of about 20%.[14] A standard Metropolis algorithm is employed in our simulations. One Monte Carlo step (MCS) consists of $0.8 \times L_x \times L_y \times L_z$ trials of reptation, local, and growing/shrinking moves, each of which occurs with the same probability. In general, we discard the first 100 000 MCS for equilibration, then make a run of at least 500 000 MCS while collecting data every 5 MCS.

As in our previous work,[14] we employ symmetric diblock copolymers of chain length $N = 24$. We set the reduced temperature to be $T^* \equiv k_BT/\epsilon_{A-B} = 2.3$, where k_B is the Boltzmann constant and T the absolute temperature. We also set the reduced chemical potential at $\mu^* \equiv \mu/(k_BT) = 41.5$, where μ is the chemical potential of the system. These conditions lead to a density of the

confined films (percentage of occupied lattice sites) of around 0.8. In the bulk, the ODT of the diblock copolymer is between $T^* = 2.8-3.0$;[14] our system is therefore in the intermediate segregation regime. The characteristic period of the lamellae in the bulk under the above conditions was estimated to be $L_0 = 12$.[14] In this work, the period of the surface pattern is considered to be $L_s/L_0 = {}^1/_3$, ${}^2/_3$, 1, 1.5, and 2 (3 for one case). We use a simulation box size of $L_x = 24$, $L_y = 36$ (for $L_s/L_0 = 1.5$ and 3) or 24 (for all other values of L_s/L_0). The film thickness D varies from L_0 to $3L_0$ ($6L_0$ for three cases). The strength of preference of the upper homogeneous surface α_H varies from 0 to 2.

2.3. Characterization of Morphology. In this section we define some of the terminology used to characterize the morphology of thin films on the chemically heterogeneous surfaces.

2.3.1. Basic Morphology. Four types of basic morphology are observed in this work: parallel lamellae, perpendicular lamellae, transposed perpendicular lamellae, and checkerboard. Other types of morphology in the confined thin films can be considered as combinations of these. For lamellar structures, we can use the normal to the A−B interfacial plane (referred to as the "normal of the lamellae") to represent the orientation of the lamellae. Parallel lamellae are denoted by the symbol ≡; their normal is parallel to the z axis. Figure 2a shows one bilayer of parallel lamellae. As shown in Figure 2b, for perpendicular lamellae, their normal is parallel to the y axis. The symbol $|||_s$ denotes perpendicular lamellae complying with the lower surface pattern (thus having period L_s), and ||| denotes perpendicular lamellae of period L_0. As shown in Figure 2c, the normal of the transposed perpendicular lamellae is parallel to the x axis (while the surface pattern is along the y direction). In this paper, all the transposed perpendicular lamellae have period L_0, and are denoted by the symbol $|||^T$. The checkerboard morphology has period L_s in the y direction. Such morphology is denoted by the symbol +[m], where m is the number of chain layers along the z direction (as discussed below, in checkerboard morphology diblock copolymer chains are mainly perpendicular to the patterned surface). Figure 2d shows the +[2] morphology.

2.3.2. Order Parameter Profile. To characterize the morphology observed in our simulations, we calculate the order parameter profiles along the x, y and z directions. The order parameter profile along the x direction, for example, is $\langle \rho_A(x) - \rho_B(x) \rangle$, where $\rho_A(x)$ is the percentage of lattice sites occupied by A segments in the cross section of a $y-z$ plane at a given x, and $\langle\rangle$ represents an average over all of the collected configurations (after equilibration). For a lamellar structure, the order parameter profile along the direction of its normal features the spatially alternative arrangement of A-rich and B-rich layers. Since the density of our films is around 0.8, the maximum and minimum values of the order parameter profile along this direction should be close to 0.8 (in A-rich layers) and −0.8 (in B-rich layers), respectively, and the period of the oscillation of the order parameter profile is equal to the lamellar period, provided that a lamellar structure is well developed (along this direction) in our simulation.

When there is a translational symmetry along the direction of the normal of the lamellae, the A−B interfaces have no preferred location (in the fixed coordinates) along this direction. Therefore, to keep the oscillating feature of the order parameter profiles along this direction from being smeared out by the average (in the fixed coordinates), we align the order parameter profile of each configuration by starting from the cross section where the maximum value of the order parameter profile occurs. For example, in the case of transposed perpendicular lamellae forming along the x direction, in which PBC are imposed, $\rho_A(x^*) - \rho_B(x^*)$ always has its maximum value at $x^* = 1$ for each collected configuration, where x^* is the aligned coordinate. Such an aligned order parameter profile, denoted by $\langle \rho_A(x^*) - \rho_B(x^*) \rangle$, captures lamellar features unequivocally. Because of morphology irregularities, the aligned order parameter profiles have a small positive value in the region near $x^* = 1$ even if there is no lamellar structure along the x direction at all. This, however, does not affect our analysis qualitatively. Similarly, the

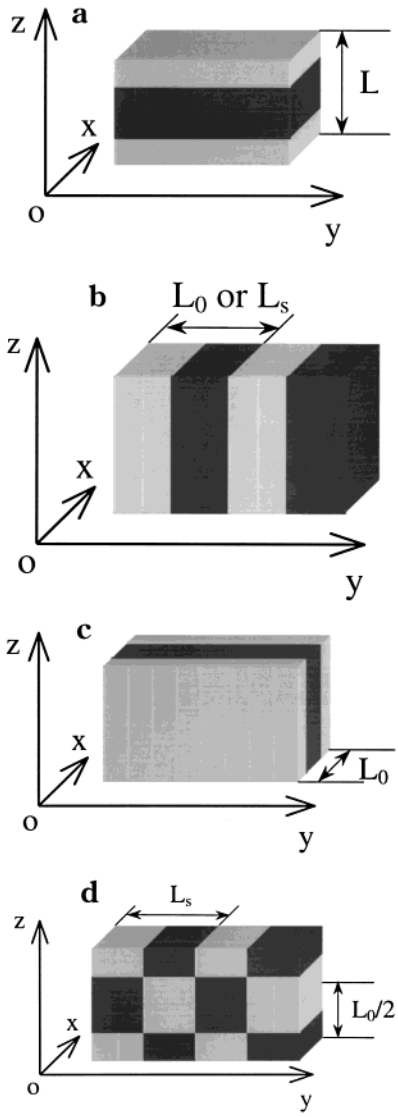

Figure 2. Illustration of the four types of basic morphology observed in Monte Carlo simulations. Light regions represent A blocks, and dark regions represent B blocks. (a) Parallel lamellae, denoted by ≡. L denotes the confined lamellar period (here shows one bilayer of parallel lamellae). (b) Perpendicular lamellae of bulk lamellar period L_0 (denoted by |||) or surface pattern period L_s (denoted by $|||_s$). (c) Transposed perpendicular lamellae (always having a period L_0), denoted by $|||^T$. (d) Checkerboard morphology, denoted by +[m], where m is the number of the layers of chains perpendicular to the surfaces in the confined film (here $m = 2$).

aligned order parameter profiles along the y direction, $\langle \rho_A(y^*) - \rho_B(y^*) \rangle$, always have their maximum value at $y^* = 1$, regardless of surface configuration. In this paper, the order parameter profiles along the x direction are always aligned, while those along the z direction are not aligned. The order parameter profiles along the y direction are either aligned or unaligned, depending on the purpose of our analysis.

2.3.3. Orientation Profiles of Diblock Copolymer Chains. We define an orientation vector pointing from the center-of-mass of A block to the center-of-mass of B block (on the same molecule) to describe the orientation of a diblock copolymer chain. Since we are only concerned with the orientation of chains relative to the surfaces, we calculate $\langle|\cos\theta(z)|\rangle_b$ and $\langle\cos\theta(z)\rangle_b$, where $0 \le \theta(z) \le \pi$ is the angle between the direction of the z axis and the orientation vector of a chain whose center-of-mass (for the whole chain) is located between $z - 0.5$ and $z + 0.5$ ($z = 1, 2, ..., L_z$) in configuration of the system; $\langle\rangle_b$ is an average over all such chains in each collected configuration, and over 1000 successively collected configurations (which correspond to 5000 MCS for the simulations in the expanded grand-canonical ensemble). Such an average can provide us with qualitative and "instant" information on some locally stable morphology.

In perpendicular or transposed perpendicular lamellae, chains are mainly parallel to the surfaces, and therefore $\theta(z) \approx \pi/2$, $\langle|\cos\theta(z)|\rangle_b \approx 0$, and $\langle\cos\theta(z)\rangle_b \approx 0$. In parallel lamellae, chains are mainly perpendicular to the surfaces, and therefore $\theta(z) \approx 0$ or π, $\langle|\cos\theta(z)|\rangle_b \approx 1$, and $\langle\cos\theta(z)\rangle_b \approx 1$ (in the case of $\theta(z) \approx 0$) or -1 (in the case of $\theta(z) \approx \pi$). In the checkerboard morphology, chains are also mainly perpendicular to the surfaces, and thus $\theta(z) \approx 0$ or π, $\langle|\cos\theta(z)|\rangle_b \approx 1$, but $\langle\cos\theta(z)\rangle_b \approx 0$ due to the average over all the chains with $\theta(z) \approx 0$ and π. From $\langle|\cos\theta(z)|\rangle_b$ and $\langle\cos\theta(z)\rangle_b$, we can distinguish among these types of morphology. Because of morphology irregularities, we choose $\langle|\cos\theta(z)|\rangle_b = (1/\pi)\int_0^\pi |\cos\theta|\, d\theta = 2/\pi$ as the criterion between the perpendicular and parallel orientations of the chains. This quantity is represented by a horizontal dashed line in subsequent figures of chain orientation profiles. Since copolymer molecules cannot penetrate the hard surfaces, chains close to the surfaces prefer to assume a parallel orientation. Thus, $\langle|\cos\theta(z)|\rangle_b$ and $\langle\cos\theta(z)\rangle_b$ are almost 0 near the surface. This is referred to as the "hard-surface effects".[14] Such effects induce the formation of perpendicular lamellae near neutral surfaces; see ref 14 for details.

2.3.4. Center-of-Mass Distribution of Chains along the *z* Direction. We also calculate the chain center-of-mass distribution along the z direction, denoted by $\langle D(z)\rangle_b$. For a collected configuration of the system, $D(z) \equiv N_c(z)/N_c$, where $N_c(z)$ is the number of chains whose center-of-mass (for the whole chain) lies between $z - 0.5$ and $z + 0.5$ ($z = 1, 2, ..., L_z$), and N_c is the total number of chains in the system.[14] For perpendicular lamellae and transposed perpendicular lamellae, chains are uniformly distributed along the z direction in the confined film, except near the surfaces. Because of the entropy loss of chains near the hard surfaces, few chains have their center-of-mass very close to the surfaces. Thus, $\langle D(z)\rangle_b$ is almost 0 at $z = 1$ and L_z, and it should show a peak at a distance slightly away from the surfaces (usually at $z = 2$ and $L_z - 1$). This is also a manifestation of the "hard-surface effects".[14] For parallel lamellae and checkerboard morphology, the center-of-mass distribution fluctuates along the z direction; most chains have their center-of-mass in the middle of each chain layer, and only a few chains have their center-of-mass between two neighboring chain layers.

Table 1. Values of $\sigma(x,y,z)$ Used in Calculating the Pattern Index Profiles

$\sigma(x,y,z)$		segment type at (x,y,z)		
		vacancy	A	B
type of lower surface site at (x,y)	sA	0	1	−1
	sB	0	−1	1

2.3.5. Pattern Index Profile. In this paper all lower surfaces are stripe-patterned. We calculate the pattern index profile $\langle P(z)\rangle_b$ in the cross section of the $x-y$ plane at each z. For a collected configuration of the system, we define the pattern index at a given z as

$$P(z) = \frac{1}{L_x L_y}\sum_{x=1}^{L_x}\sum_{y=1}^{L_y}\sigma(x,y,z)$$

where the value of $\sigma(x,y,z)$ is listed in Table 1. If the pattern in the cross section is completely in-phase with the lower surface pattern, then $\langle P(z)\rangle_b \approx 0.8$. Similarly, if the pattern in the cross section is completely out-of-phase with the lower surface pattern, then $\langle P(z)\rangle_b \approx -0.8$.

3. Results and Discussion

3.1. Morphology between Patterned-Neutral Surfaces. The observed morphology of the confined thin films is summarized in Table 2. For most cases, we observe some mixed morphology within the film. For example, $|||_s(0.21)-|||$ in Table 2 represents the mixed morphology of perpendicular lamellae complying with the surface pattern ($|||_s$) near the lower patterned surface and perpendicular lamellae of period L_0 ($|||$) near the upper neutral surface. The number in the parentheses (0.21) is the ratio of height of the lower morphology in the z direction to L_0. Note that due to the complexity of the observed morphology, this number only provides a rough estimation.

3.1.1. Commensurate Systems: $L_s/L_0 = 1$. When the surface pattern period L_s is commensurate with the bulk lamellar period L_0, that is when $L_s = L_0$, we observe perpendicular lamellae complying with the surface pattern ($|||_s$) throughout the entire film, for all surface separations studied in this work. This is consistent with refs 6, 7, and 9. Figure 3a gives a representative configuration of the morphology for $D/L_0 = 2$; it shows the six surfaces of our simulation box. From the figure, we can see that the morphology is perpendicular lamellae throughout the film. The order parameter profiles along the x, y and z directions are shown in Figure 3b, which indicate the well-developed lamellar structure along the y direction. The maximum and minimum value of $\langle \rho_A(y) - \rho_B(y)\rangle$ are close to 0.8 and −0.8, respectively. Also, from the unaligned order parameter profile along the y direction, we can see that the perpendicular lamellae are in-phase with the lower surface pattern. The chain orientation profiles shown in Figure 3c confirm the parallel orientation of copolymer chains throughout the entire film. This is in agreement with hypotheses advanced in refs 6 and 7. In the chain orientation and center-of-mass distribution

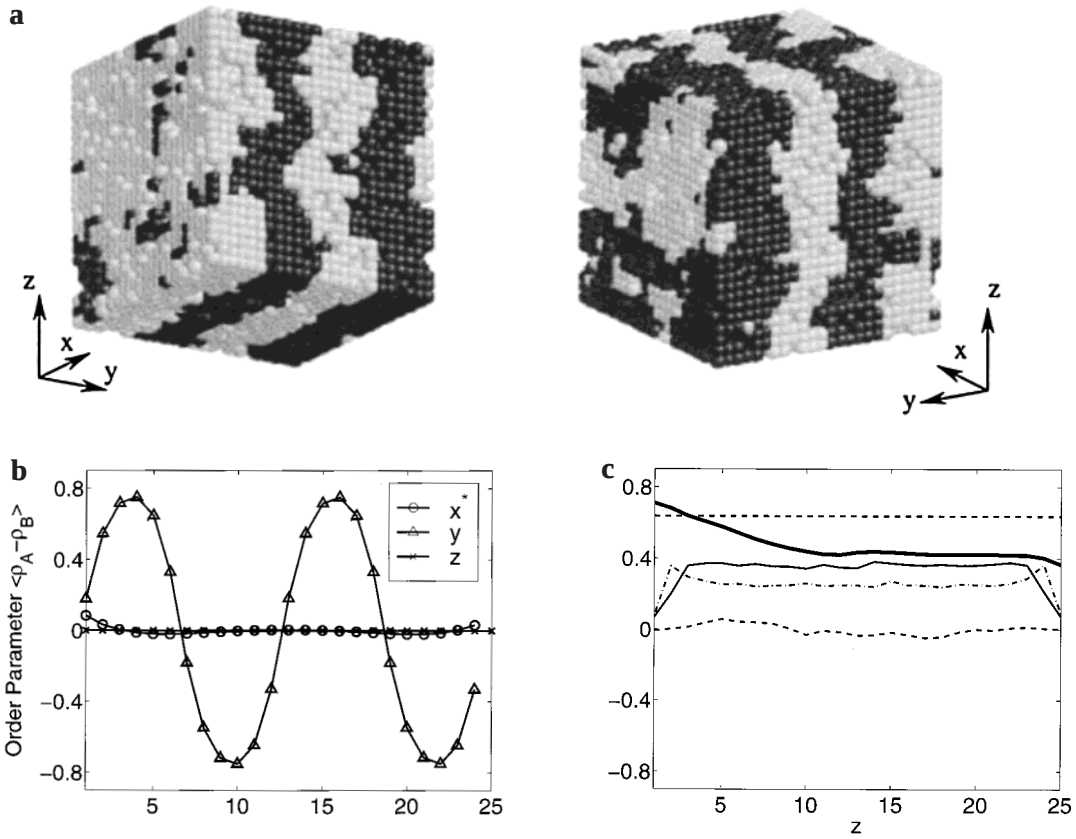

Figure 3. $|||_s$ morphology between patterned-neutral surfaces at $L_s/L_0 = 1$ and $D/L_0 = 2$. Perpendicular lamellae complying with the lower surface pattern ($|||_s$) form throughout the entire film. (a) Representative configuration of the system from a Monte Carlo simulation. The six surfaces of the simulation box are shown in the figure, where light regions represent A blocks and dark regions represent B blocks. (b) Order parameter profiles. The horizontal axis represents the coordinates as indicated in the legend for each curve. (c) Chain orientation, center-of-mass distribution, and pattern index profiles. The thin solid line represents $\langle|\cos\theta(z)|\rangle_b$. The horizontal dashed line represents the criterion between the perpendicular and parallel orientations of chains: $\langle|\cos\theta(z)|\rangle_b = (1/\pi)\int_0^\pi |\cos\theta|\, d\theta = 2/\pi$. The dashed line represents $\langle\cos\theta(z)\rangle_b$. The dash−dotted line represents $\langle D(z)\rangle_b \times L_z/4$ (the factor $L_z/4$ is used to re-scale the curve). The thick solid line represents $\langle P(z)\rangle_b$.

Table 2. Morphology of Symmetric Diblock Copolymer Thin Films Confined between Patterned-Neutral Surfaces[a]

	L_s/L_0					
D/L_0	$^1/_3$	$^2/_3$	1	1.5	2	3
1	$\|\|\|$ $\|\|\|^T$	$\|\|\|_s(0.21)-\|\|\|$ $\|\|\|_s(0.23)-\|\|\|^T$	$\|\|\|_s$	$\|\|\|_s(0.23)-\|\|\|$	+[2]	N.A.
1.5	$\|\|\|$	$\|\|\|_s(0.23)-\|\|\|$ $\|\|\|_s(0.24)-\|\|\|^T$	$\|\|\|_s$	$\|\|\|_s(0.24)-\|\|\|$	+[1](0.45)−$\|\|\|$ +[1](0.47)−$\|\|\|^T$	N.A.
2	$\|\|\|$	$\|\|\|_s(0.23)-\|\|\|$ $\|\|\|_s(0.25)-\|\|\|^T$	$\|\|\|_s$	$\|\|\|_s(0.25)-\|\|\|$	+[1](0.44)−$\|\|\|$	N.A.
2.5	$\|\|\|$	$\|\|\|_s(0.23)-\|\|\|$ $\|\|\|_s(0.27)-\|\|\|^T$	$\|\|\|_s$	$\|\|\|_s(0.24)-\|\|\|$	+[1](0.47)−$\|\|\|$	N.A.
3	$\|\|\|$ $\|\|\|^T$	$\|\|\|_s(0.27)-\|\|\|$	$\|\|\|_s$	$\|\|\|_s(0.28)-\|\|\|$	+[1](0.53)−$\|\|\|$ +[1](0.52)−$\|\|\|^T$	N.A.
6	N.A.	N.A.	$\|\|\|_s$	$\|\|\|_s-\|\|\|^T$	N.A.	+[1]−$\|\|\|^T$

[a] The symbol $|||$ denotes perpendicular lamellae of period L_0; $|||_s$ denotes perpendicular lamellae complying with the surface pattern; $|||^T$ denotes transposed perpendicular lamellae with period L_0; ≡ denotes parallel lamellae; +[m] denotes checkerboard morphology, where m is the number of chain layers along the z direction in the confined films. The mixed morphology, for example, $|||_s(0.21)-|||$ represents $|||_s$ near the lower patterned surface and $|||$ near the upper neutral surface, where the number in parentheses (0.21) is the ratio of the height of the lower morphology in the z direction to L_0. Different types of morphology under the same L_s/L_0 and D/L_0 were observed in distinct runs, with the only difference being the random number generator seeds. N.A. represents the case where no simulation has been conducted.

profiles shown in Figure 3c, we see a manifestation of the hard-surface effects discussed in ref 14.

In previous work we found that perpendicular lamellae form when copolymers are confined between two neutral surfaces, for all surface separations.[14] Experimental results show that the ordering of perpendicular lamellae confined between two homogeneous surfaces is short-ranged.[1−3] Employing a stripe-patterned surface with $L_s = L_0$ enhances the formation of perpendicular lamellae, and also aligns (over a macroscopic scale) the perpendicular lamellae to be in-phase with the surface pattern by the strong surface−block interactions. This can be seen from the pattern index profile shown in Figure 3c. Although there is some decay in $\langle P(z)\rangle_b$ as z

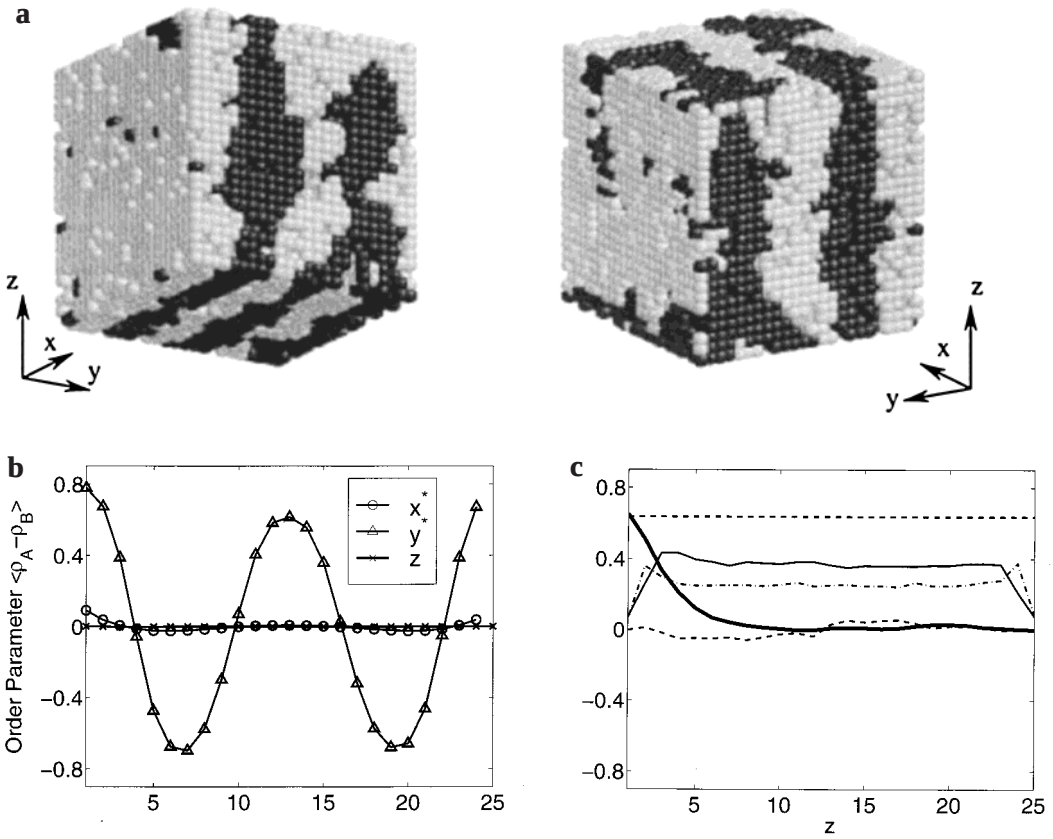

Figure 4. $|||_s-|||$ morphology between patterned-neutral surfaces at $L_s/L_0 = {}^2/_3$ and $D/L_0 = 2$. Perpendicular lamellae complying with the lower surface pattern ($|||_s$) form near the patterned surface, and perpendicular lamellae of period L_0 ($|||$) form near the upper neutral surface. Refer to Figure 3 for more explanations.

increases (from about 0.7 at $z = 0$ to about 0.4 at $z >$ 10), the pattern throughout the entire film is basically in-phase with the lower surface pattern. ($\langle P(z)\rangle_b \approx 0.4$ indicates that about 60% of lattice sites are in-phase and 20% are out-of-phase with the lower surface pattern, while the remaining 20% are vacancies.) The decay is due to the relatively weak block−block interactions compared to the surface−block interactions. The effect of the lower stripe-patterned surface with $L_s = L_0$ was also seen in experiments.[4]

3.1.2. Incommensurate Systems: $L_s/L_0 = {}^2/_3$ and 1.5. When L_s differs from L_0 by a small amount, e.g. $L_s/L_0 = {}^2/_3$ and 1.5, we observe some mixed morphology of $|||$ (or $|||^T$) near the upper neutral surface and $|||_s$ near the lower patterned surface. Figure 4 shows the $|||_s-|||$ morphology for $L_s/L_0 = {}^2/_3$ and $D/L_0 = 2$. We obtain a similar type of morphology for all other surface separations. Note that the aligned order parameter profile in the y direction is actually the superposition of the corresponding order parameter profiles in $|||$ and $|||_s$ of different periods. This can be seen from the differences among the absolute values of the extreme values of $\langle \rho_A(y^*) - \rho_B(y^*)\rangle$. Because in this case there is a translational symmetry along the y direction for the upper $|||$ morphology, aligning the order parameter profile in the y direction for each collected configuration is necessary to keep the main feature of such a superposition from being smeared out by the average. The height of the lower $|||_s$ morphology in the z direction is roughly estimated from the difference between 0.8 and the extreme value of $\langle \rho_A(y^*) - \rho_B(y^*)\rangle$ at $y^* = 13$. This height is small, as shown in Table 2. From the pattern index profile we can also see that the lower surface pattern is only preserved over a short range from the surface, and $\langle P(z)\rangle_b$ decays rapidly to 0 in $|||$.

In some distinct runs for $L_s/L_0 = {}^2/_3$ (with the only difference being the random number generator seeds), we observe some mixed morphology $|||_s-|||^T$. Such a morphology for $D/L_0 = 2$ is shown in Figure 5. A similar type of morphology is also found for several other surface separations, as shown in Table 2. From the order parameter profiles we can see that perpendicular lamellae of period L_0 and L_s form along the x and y directions, respectively. $|||_s$ is in-phase with the lower surface pattern. The height of $|||_s$ in the z direction, roughly estimated from the extreme values of $\langle \rho_A(y) - \rho_B(y)\rangle$, is small and almost the same as that in the $|||_s-|||$ morphology. The chain orientation, center-of-mass distribution and pattern index profiles shown in Figure 5c are similar to those in Figure 4c. The small values of $\langle|\cos\theta(z)|\rangle_b$ confirm the parallel orientation of chains throughout the entire film. The $|||_s-|||^T$ morphology has almost the same block−block interfacial energy as the $|||_s-|||$ morphology and occurs as a local energy minimum of our system. The energy barrier between these two types of morphology cannot be overcome by our algorithms during the course of a single simulation run. This is why we see them in distinct runs.

The $|||_s-|||$ morphology for $L_s/L_0 = 1.5$ and $D/L_0 = 1$ is shown in Figure 6. In this case, the superposition of the aligned order parameter profiles along the y direction in $|||$ and $|||_s$ can be seen more clearly. The height of the $|||_s$ morphology in the z direction is roughly estimated from the difference between −0.8 and the extreme value of $\langle \rho_A(y^*) - \rho_B(y^*)\rangle$ at $y^* = 19$. Again, this height is small. We obtain a similar type of morphology

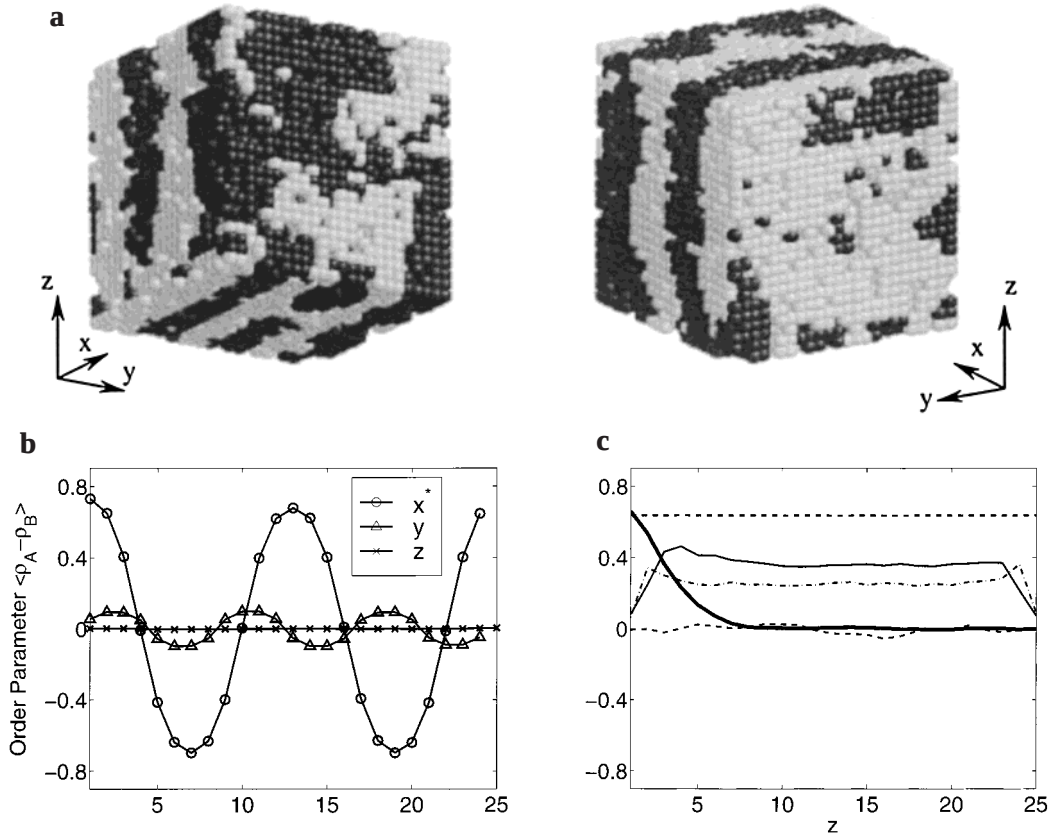

Figure 5. $|||_s-|||^T$ morphology between patterned-neutral surfaces at $L_s/L_0 = {}^2/_3$ and $D/L_0 = 2$. Perpendicular lamellae complying with the lower surface pattern ($|||_s$) form near the patterned surface, and transposed perpendicular lamellae of period L_0 ($|||^T$) form near the upper neutral surface. Refer to Figure 3 for more explanations.

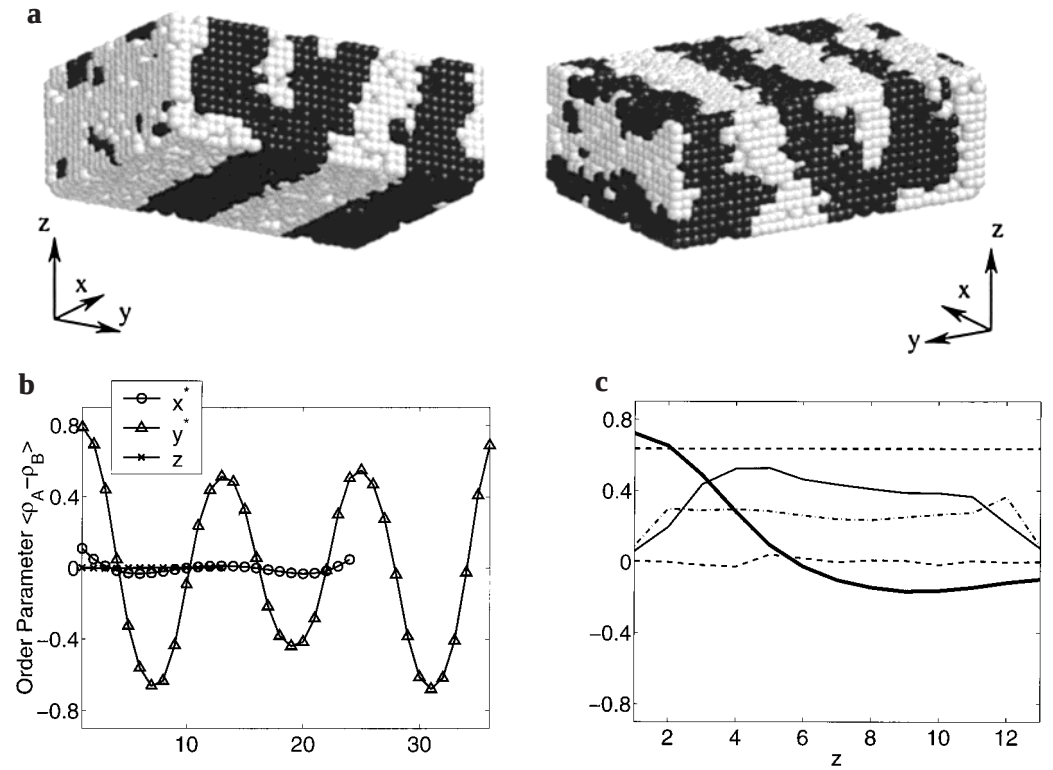

Figure 6. $|||_s-|||$ morphology between patterned-neutral surfaces at $L_s/L_0 = 1.5$ and $D/L_0 = 1$. Perpendicular lamellae complying with the lower surface pattern ($|||_s$) form near the patterned surface, and perpendicular lamellae of period L_0 ($|||$) form near the upper neutral surface. Refer to Figure 3 for more explanations.

for all other surface separations. We note that the peak of $\langle D(z)\rangle_b$ (at $z = 2$) shown in Figure 6c is different from the peak caused by the hard-surface effects (at $z = 12$). Also $\langle P(z)\rangle_b$ has a slightly different shape (showing a

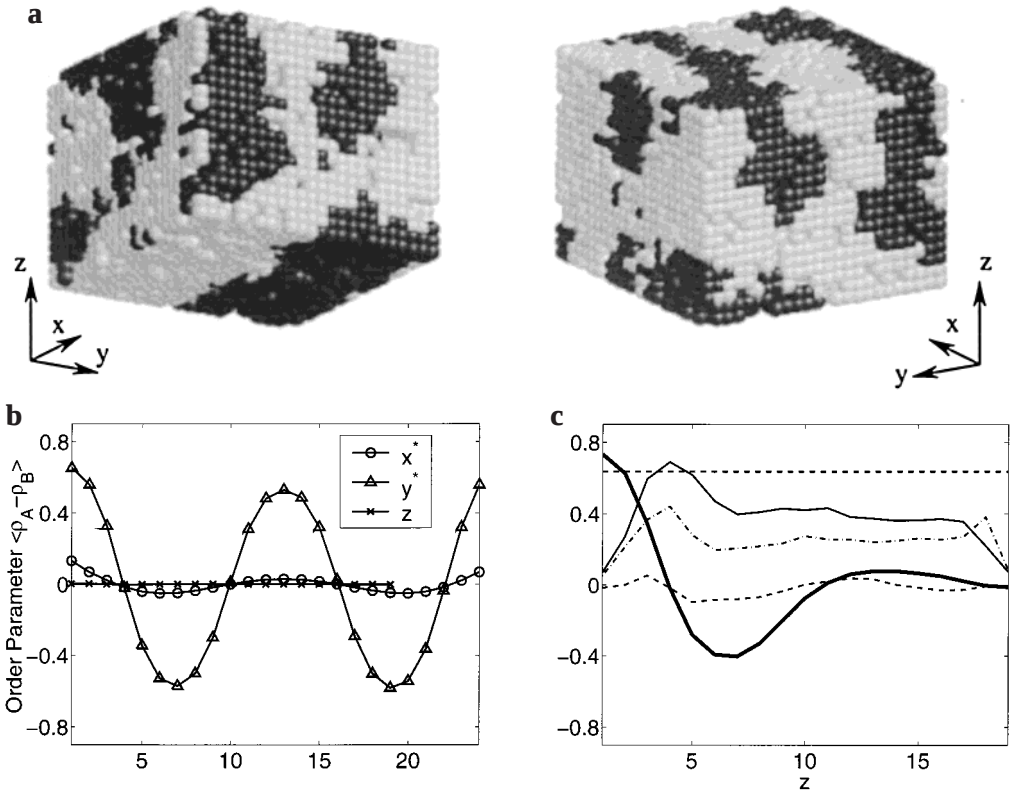

Figure 7. +[1]−||| morphology between patterned-neutral surfaces at $L_s/L_0 = 2$ and $D/L_0 = 1.5$. One layer of checkerboard morphology (+[1]) forms near the lower patterned surface, and perpendicular lamellae of period L_0 (|||) form near the upper neutral surface. Refer to Figure 3 for more explanations.

negative minimum value at $z = 9$) from that for the case $L_s/L_0 = {}^2/_3$. These findings point to the complex conformation that chains adopt as a combination of $|||_s$ and ||| in this case.

We have seen that perpendicular lamellae of period L_0 (||| or $|||^T$) are induced near neutral surfaces by the hard-surface effects.[14] For the lower patterned surface where L_s is different from L_0 (but not too much), the strong surface−block interactions stretch or compress the diblock copolymers near the patterned surface to form perpendicular lamellae complying with the surface pattern ($|||_s$). Forming the $|||_s$ morphology throughout the entire film would cost too much elastic energy (conformational entropy) to change the confined lamellar period to L_s, while forming ||| (or $|||^T$) near the patterned surface would cost too much surface−block interfacial energy. The competition between these two factors leads to the mixed morphology $|||_s$−||| (or $|||_s$−$|||^T$), at the lesser cost of increasing the block−block interfacial energy between $|||_s$ and ||| (or $|||^T$). We can also see from Table 2 that the height of $|||_s$ is almost constant regardless of the surface separation, which is a direct result of such a competition. Refer to ref 13 for a detailed discussion.

The $|||_s$−||| morphology observed in our simulations is similar to that reported by Petera and Muthukumar[9] in their self-consistent field calculations of symmetric diblock copolymers between patterned-neutral surfaces with $L_s/L_0 = 0.75$ and $D/L_0 = 2$. (Since they performed two-dimensional calculations, they did not obtain the $|||_s$−$|||^T$ morphology.) However, the $|||_s$−≡ morphology they obtained (in the case of $L_s/L_0 = 0.75$ and $D/L_0 = 3$) contradicts our findings, and may not represent the global minimum of the free energy of the system. The formation of the upper parallel lamellae (≡) is not preferred by the hard and neutral surface on the top. This may be the reason why they observed a change of the upper morphology from the parallel lamellae to a perpendicular orientation when using different grid resolutions and tolerance in their calculations.[9]

The $|||_s$−||| morphology observed in our simulations for $L_s/L_0 = 1.5$ and $D/L_0 = 1$ (shown in Figure 6) is different from the morphology suggested by Chen and Chakrabarti[6,7] in their Cahn−Hilliard calculations for symmetric diblock copolymers between patterned-neutral surfaces with $L_s/L_0 \approx 1.5$ and $D/L_0 = 1$. The morphology found by these authors can be represented as +*[1]−$|||_s$, where the one layer of checkerboard near the lower patterned surface is *vertically* (along the *z* direction) stretched about 50%, and the upper perpendicular lamellae are laterally stretched about 50% to comply with the inverted (by the one layer of checkerboard) lower surface pattern. Although in the strong segregation regime and with weak surface−block interactions (i.e., under the conditions in their calculations[6,7]) the +[1]−||| morphology (or even the +[1]−$|||_s$ morphology in order to reduce the block−block interfacial energy between +[1] and the upper perpendicular lamellae) could be possible, it would be difficult to explain why the checkerboard has to be *vertically* stretched. Even if the elastic energy (conformational entropy) cost for creating such an extended layer is not too large, as argued by Chen and Chakrabarti[6,7], the $|||_s$ morphology (throughout the entire film) would have a lower free energy than the morphology they proposed. Their morphology could therefore correspond to a local free energy minimum, as opposed to the global minimum.

3.1.3. Incommensurate Systems: $L_s/L_0 = {}^1/_3$ and 2. We have seen that there exist some limits within

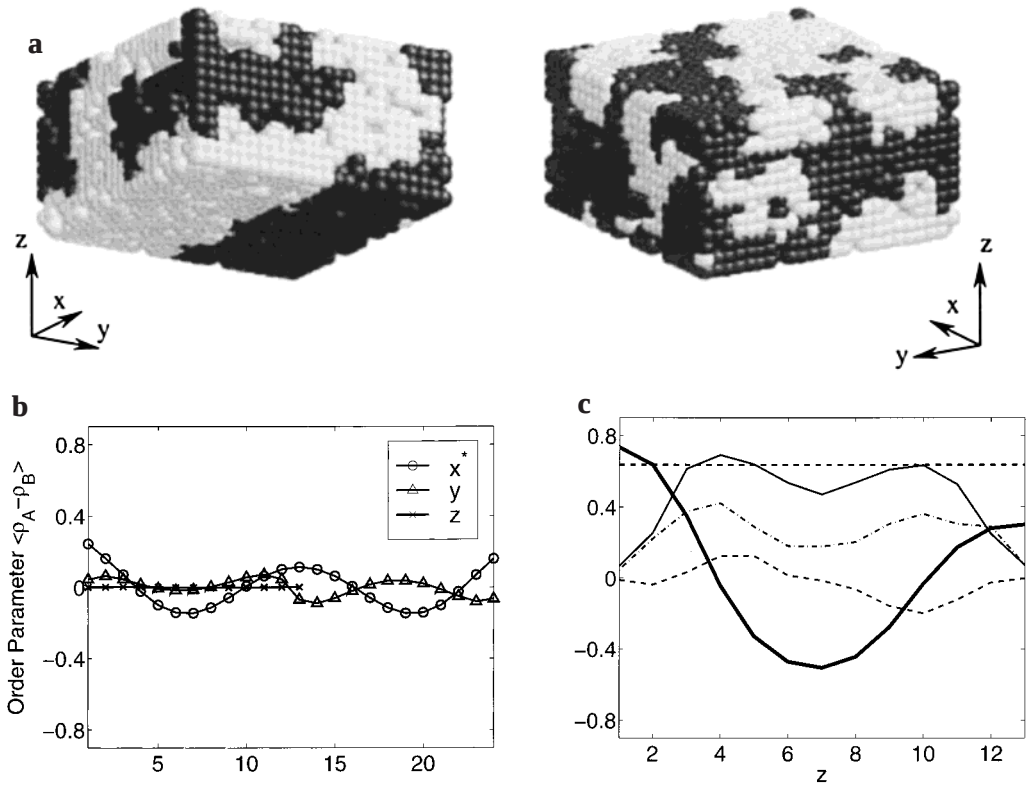

Figure 8. +[2] morphology between patterned-neutral surfaces at $L_s/L_0 = 2$ and $D/L_0 = 1$. About two layers of checkerboard morphology (+[2]) form within the confined film. Refer to Figure 3 for more explanations.

which confined lamellae can be stretched or compressed; beyond these limits, copolymer chains change their orientation, instead of being excessively stretched or compressed.[14] If L_s/L_0 is too large, for example, in the case of $L_s/L_0 = 2$, it would cost too much elastic energy (conformational entropy) for chains to be stretched while orienting parallel to the surfaces (i.e., to form $|||_s$ near the patterned surface). Instead, most chains change their orientation from parallel to perpendicular to the surfaces, thereby leading to the checkerboard near the lower patterned surface. However, ||| (or $|||^T$) is still preferred near the upper neutral surface due to the hard-surface effects.[14] Therefore, as shown in Table 2, for most cases we observe the mixed morphology +[1]−||| (or +[1]−$|||^T$).

Figure 7 shows the +[1]−||| morphology for $L_s/L_0 = 2$ and $D/L_0 = 1.5$. Both the peak of $\langle|\cos\theta(z)|\rangle_b$ and the peak of $\langle D(z)\rangle_b$ at $z = 4$, shown in Figure 7c, indicate one layer of chains perpendicular to the surfaces. The change of $\langle P(z)\rangle_b$ from about 0.7 at $z = 1$ (in-phase) to −0.4 at $z = 7$ (out-of-phase) also indicates the existence of +[1] near the lower patterned surface. Note that the difference between these two values of $\langle P(z)\rangle_b$ shows that +[1] is not too regular. On the other hand, the aligned order parameter profile along the *y* direction shows that ||| forms near the upper neutral surface. The height of ||| is roughly estimated from the extreme values of $\langle\rho_A(y^*) - \rho_B(y^*)\rangle$, which in turn gives the height of +[1] reported in Table 2. As shown in Table 2, we also observe the +[1]−$|||^T$ morphology in several distinct runs.

Forming the checkerboard increases the block−block interfacial energy, but chains are no longer stretched. From Table 2 we can see that the height of +[1] in the *z* direction is almost $L_0/2$, which corresponds to one layer of chains perpendicular to the surfaces without being stretched. As discussed above, forming the upper ||| (or $|||^T$) morphology is preferred by the hard and neutral surface on the top. Furthermore, forming ||| (or $|||^T$), instead of more layers of checkerboard, would avoid the frustration between *D* and $L_0/2$ when D/L_0 is not half an integer. It would also decrease the block−block interfacial energy in the system when $D/L_0 > 1$. Refer to ref 13 for a detailed discussion.

For $L_s/L_0 = 2$ and $D/L_0 = 1$, we observe some morphology consisting of basically two layers of checkerboard (+[2]), as shown in Figure 8. The chain orientation profiles, as well as the small fluctuations in the order parameter profile along the *y* direction, confirm that the upper morphology is checkerboard, instead of perpendicular lamellae. Since the top surface is neutral, the upper layer of checkerboard is not so regular as illustrated in Figure 2d. This can also be seen from $\langle P(z)\rangle_b \approx 0.3$ at $z = 13$, which suggests that about 55% of lattice sites are in-phase and 25% are out-of-phase with the lower surface pattern (the remaining 20% are vacancies). Such morphology was also found by Chen and Chakrabarti.[6, 7]

If L_s/L_0 is too small, for example, in the case of $L_s/L_0 = {}^1/_3$, forming the $|||_s$ morphology throughout the entire film would cost too much elastic energy (conformational entropy) for chains to be excessively compressed, while forming the checkerboard morphology would cost too much block−block interfacial energy. Instead, the ||| (or $|||^T$) morphology develops at the lesser cost of increasing the surface−block interfacial energy. In this case the patterned surface acts more like a homogeneous surface repelling the whole chain, and diblock copolymers almost ignore the surface pattern. The ||| morphology for $L_s/L_0 = {}^1/_3$ and $D/L_0 = 3$ is shown in Figure 9. The lower surface pattern is hardly preserved even in the immediate vicinity of the surface. This can be seen from

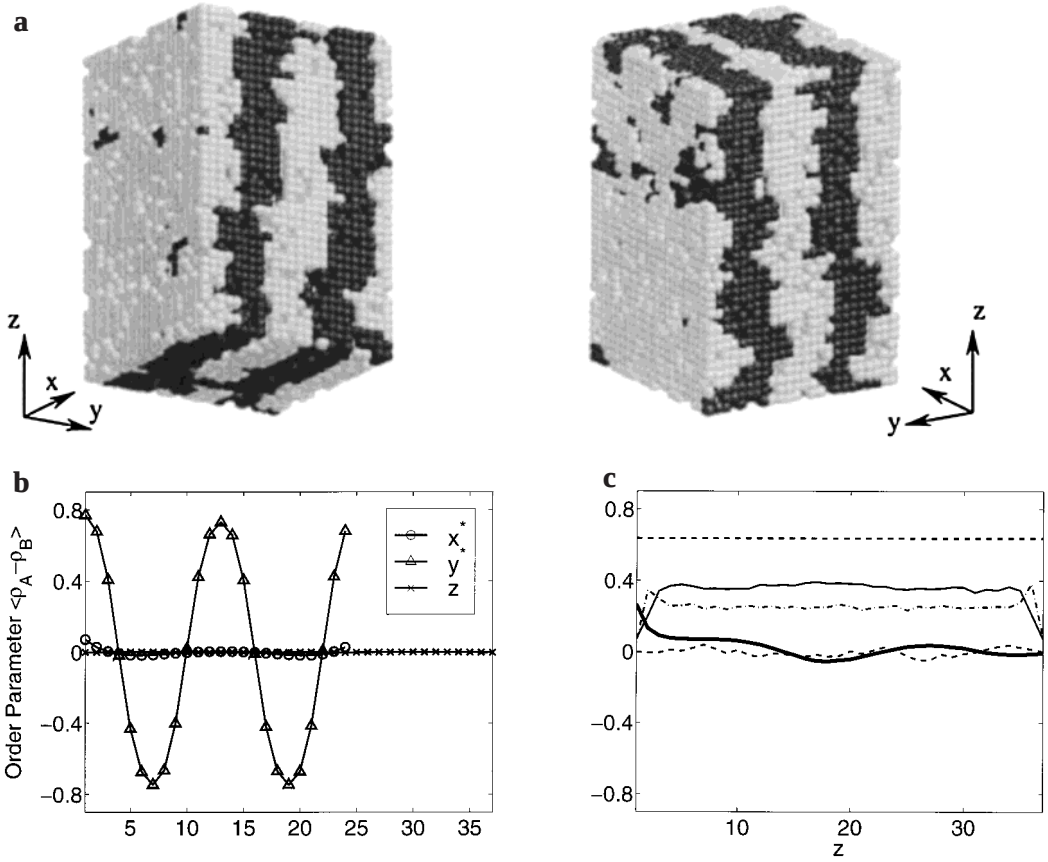

Figure 9. ||| morphology between patterned-neutral surfaces at $L_s/L_0 = {}^1/_3$ and $D/L_0 = 3$. Perpendicular lamellae of period L_0 (|||) form throughout the entire film. Refer to Figure 3 for more explanations.

$\langle P(z)\rangle_b$. The $|||^T$ morphology is also observed in our simulations, as shown in Table 2. The morphology we observe here is similar to that obtained by Chen and Chakrabarti for the case $L_s/L_0 \approx 0.4$.[7] Note that it would be difficult to achieve macroscopic ordering of the perpendicular lamellae in these systems.

For thin films confined between patterned-neutral surfaces where $L_s \geq L_0$, we have never observed the tilted lamellae reported by Petera and Muthukumar in their two-dimensional self-consistent field calculations.[9,13] As shown in Table 2, in our simulations for the cases where the film thickness and the surface pattern period are comparable to those in ref 9, i.e., $D/L_0 = 6$ and $L_s/L_0 = 1$, 1.5, and 3, the morphologies $|||_s$, $|||_s - |||^T$, and $+[1]-|||^T$ are observed, respectively. This is consistent with our results reported above. As mentioned before, ||| (or $|||^T$) is preferred by the hard and neutral surface on the top due to the hard-surface effects.[14] As shown elsewhere,[16] tilted lamellae are observed only between two patterned surfaces in our simulations.

3.2. Morphology between Patterned-Preferential Surfaces. 3.2.1. Effects of the Surface Pattern Period. In this section, the upper surface is a homogeneous and strongly preferential surface that repels B segments with the same strength of surface−block interactions as the lower patterned surface, i.e., $\alpha_H = 2$. We vary the surface pattern period and the surface separation. The observed morphology is summarized in Table 3a. Again, the number in parentheses is the ratio of height of the lower morphology in the z direction to L_0 and only provides a rough estimation due to the complexity of the observed morphology.

Table 3. Morphology of Symmetric Diblock Copolymer Thin Films Confined between Patterned−Preferential Surfaces[a]

(a) Upper Strongly Preferential Surface ($\alpha_H \equiv \epsilon_{sH-B}/\epsilon_{A-B} = 2$)

	L_s/L_0				
D/L_0	$^1/_3$	$^2/_3$	1	1.5	2
2	≡	$|||_s(0.28)-≡$	$|||_s(0.92)-≡$	$+[1]-≡$	$+[1]-≡$
2.5	≡	$|||_s(0.29)-≡$	$|||_s(1.10)-≡$	$+[1]-≡$	$+[1]-≡$

(b) Patterned-Homogeneous Surfaces with $L_s/L_0 = 1$ and Different Strengths of Preference of the Upper Homogeneous Surface

	α_H						
D/L_0	0	0.2	0.25	0.5	1	1.5	2
1	$|||_s$	N.A.	$|||_s$	$|||_s$	$|||_s(0.63)-≡$	N.A.	$|||_s(0.56)-≡$
2	$|||_s$	$|||_s$	N.A.	$|||_s$	$|||_s(0.89)-≡$	$|||_s(0.91)-≡$	$|||_s(0.92)-≡$

[a] Refer to Table 2 for more explanations.

As expected, when $L_s = L_0$ the mixed morphology $|||_s-≡$ is observed between the patterned and strongly preferential surfaces, for all surface separations studied in this work, namely $D/L_0 = 1$, 1.5, 2, 2.5, and 3. A similar type of morphology was also found by Petera and Muthukumar.[9] Figure 10 shows such mixed morphology for $L_s/L_0 = 1$ and $D/L_0 = 2$. From the order parameter profiles we can see that near the lower patterned surface perpendicular lamellae of period L_s form along the y direction and are in-phase with the surface pattern ($|||_s$). We can also see from the pattern index profile that the surface pattern is preserved through $|||_s$. The height of $|||_s$ in the z direction is roughly estimated from the extreme values of $\langle \rho_A(y) - \rho_B(y)\rangle$. On the other hand, near the upper preferential surface about one bilayer of parallel lamellae form along the z

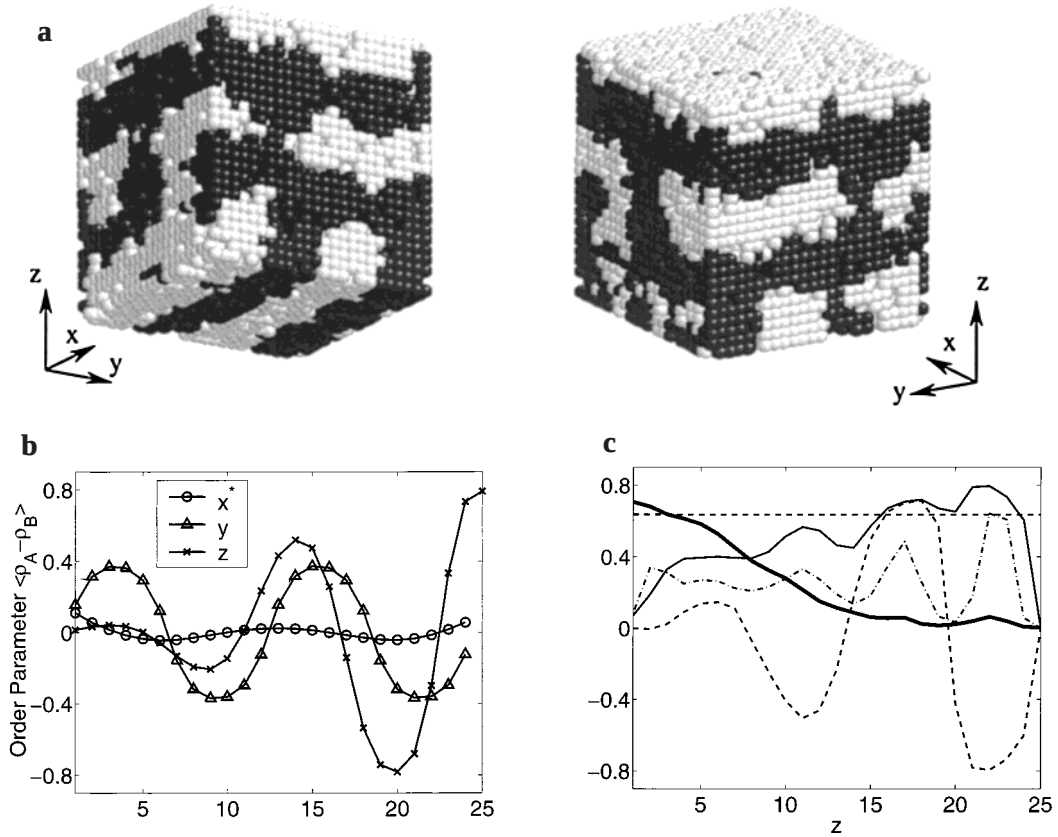

Figure 10. $|||_s-\equiv$ morphology between patterned-preferential surfaces at $L_s/L_0 = 1$ and $D/L_0 = 2$. Perpendicular lamellae complying with the lower surface pattern ($|||_s$) form near the patterned surface, and about one bilayer of parallel lamellae ($\equiv$) form near the upper homogeneous surface strongly preferring A segments. Refer to Figure 3 for more explanations.

direction. The two peaks of $\langle D(z)\rangle_b$ at $z = 17$ and 22 (where $\langle \rho_A(z) - \rho_B(z)\rangle$ is close to 0), as well as the two peaks of $\langle|\cos\,\theta(z)|\rangle_b$ with the extreme values greater than $2/\pi$ (represented by the horizontal dashed line), confirm the two layers of copolymer chains perpendicular to the surfaces. The flips of $\langle\cos\,\theta(z)\rangle_b$ in the upper part of the confined film indicate the order of A−B B−A copolymer chain layers with A blocks in the top layer segregating near the upper homogeneous surface preferring A segments. The morphology for $D/L_0 = 2.5$ is similar, except that there are basically 1.5 bilayers of parallel lamellae.

For $L_s/L_0 = {}^2/_3$, consistent with the case of patterned-neutral surfaces, we observe the mixed morphology $|||_s-\equiv$. On the other hand, as shown in Table 3a, the height of $|||_s$ in the z direction, roughly estimated from the extreme values of $\langle \rho_A(y) - \rho_B(y)\rangle$, is much smaller than that in the above cases of patterned-preferential surfaces with $L_s/L_0 = 1$. This reduces the elastic energy (conformational entropy) cost of compressing the lower perpendicular lamellae to comply with the surface pattern. As a result, the number of bilayers of parallel lamellae in the upper part of the film increases; in this case there are about 1.5 and 2 bilayers of parallel lamellae for $D/L_0 = 2$ and 2.5, respectively.

If L_s/L_0 is too small, the patterned surface acts as a homogeneous surface that repels the whole chain; the diblock copolymers would ignore the surface pattern, as discussed before. Therefore, for the case $L_s/L_0 = {}^1/_3$, we observe parallel lamellae throughout the entire film. Such morphology for $D/L_0 = 2$ is shown in Figure 11. We can see that the lower surface pattern is hardly preserved even in the immediate vicinity of the surface. There are basically two bilayers of parallel lamellae within the confined film. Note that the asymmetry of the order parameter profile in the z direction is due to the difference between the two surfaces. The morphology for $D/L_0 = 2.5$ is similar, except that there are basically 2.5 bilayers of parallel lamellae.

For $L_s/L_0 = 1.5$, we observe that one layer of checkerboard morphology forms near the lower patterned surface (this is different from that between patterned-neutral surfaces), and that parallel lamellae form near the upper surface. Such morphology for $D/L_0 = 2$ is shown in Figure 12. Both $\langle P(z)\rangle_b \approx -0.4$ at $z = 9$ and the small fluctuation of the order parameter profile along the y direction indicate the existence of +[1] near the lower patterned surface. We can also see that in this case there are about 1.5 bilayers of parallel lamellae in the upper part of the film. The morphology for $D/L_0 = 2.5$ is similar, except that there are about two bilayers of parallel lamellae. When $L_s/L_0 = 2$, we observe a similar type of morphology +[1]−$\equiv$, as expected.

3.2.2. Effects of the Strength of Preference of the Upper Homogeneous Surface. In this section, we vary the strength of preference of the upper homogeneous surface α_H within 0 and 2 for commensurate systems where $L_s/L_0 = 1$. The cases of $\alpha_H = 0$ and 2 correspond to upper neutral and strongly preferential surfaces, respectively, which we have discussed above. Two film thicknesses are studied here: D/L_0=1 and 2. The observed morphology is summarized in Table 3b. Again, the number in the parentheses is the ratio of height of the lower morphology in the z direction to L_0, and only provides a rough estimation due to the complexity of the observed morphology.

From Table 3b, we can see that an upper neutral or weakly preferential surface is necessary to obtain the

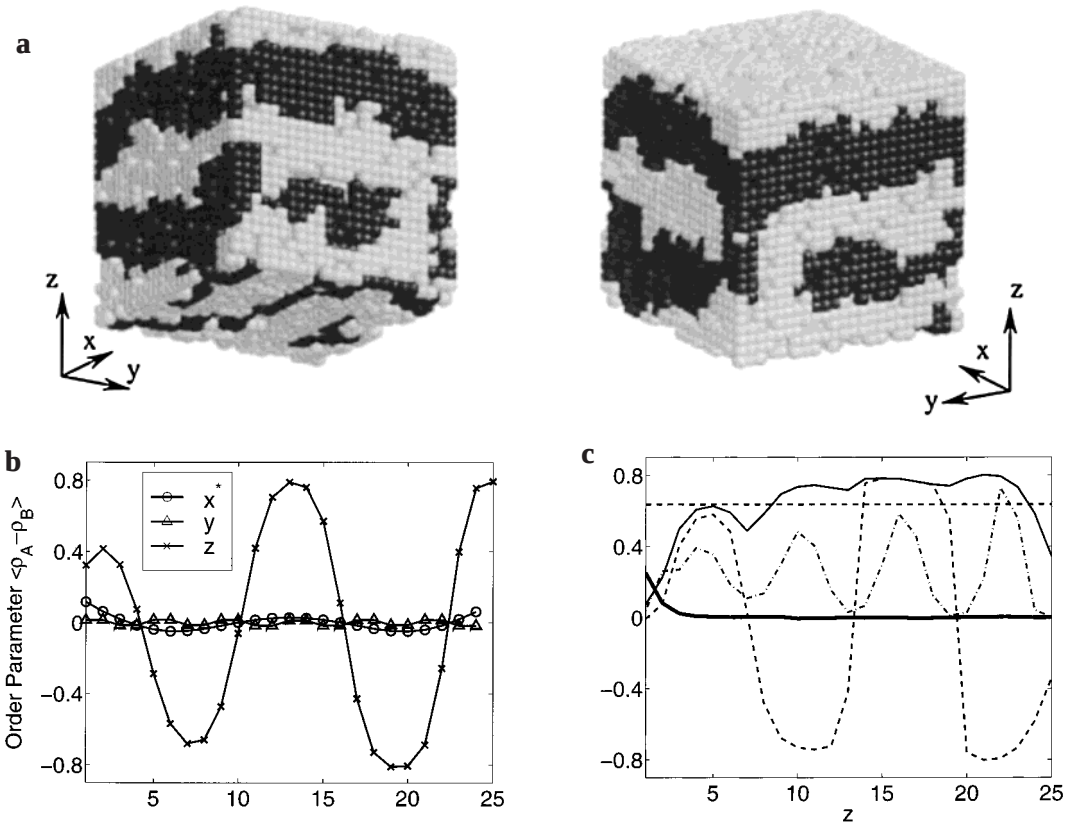

Figure 11. ≡ morphology between patterned-preferential surfaces at $L_s/L_0 = {}^1/_3$ and $D/L_0 = 2$. About two bilayers of parallel lamellae (≡) form throughout the entire film. Refer to Figure 3 for more explanations.

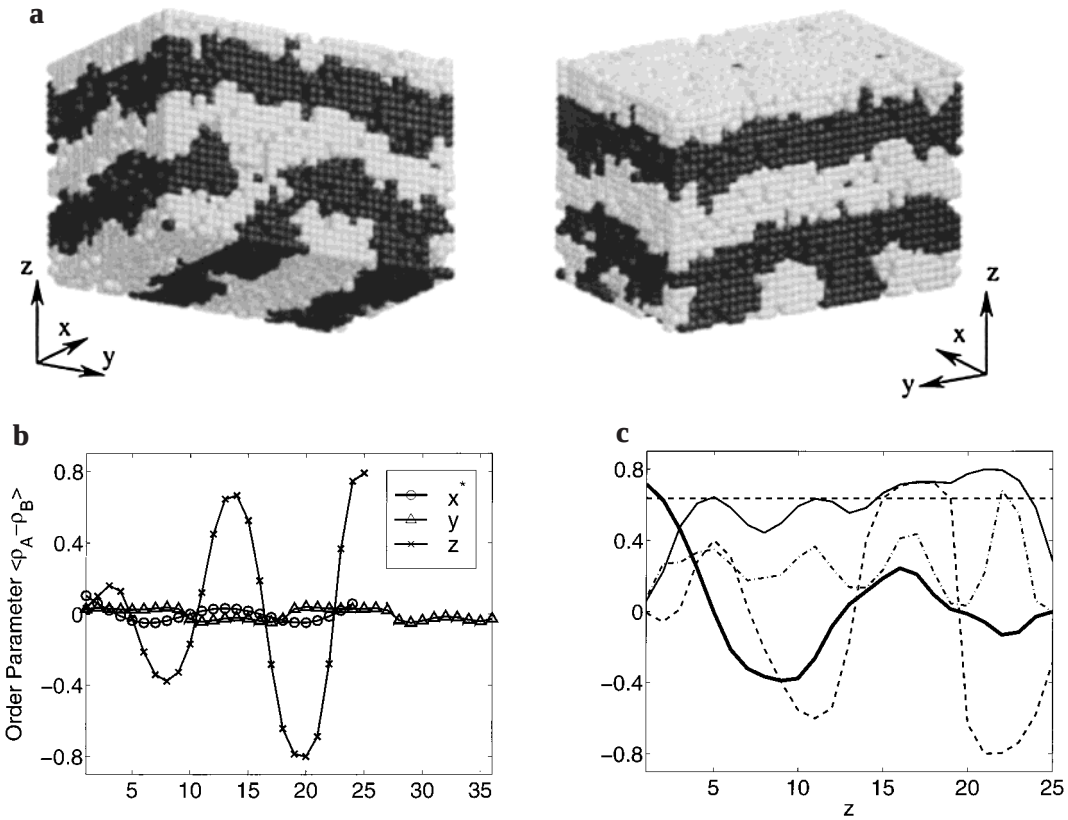

Figure 12. +[1]−≡ morphology between patterned-preferential surfaces at $L_s/L_0 = 1.5$ and $D/L_0 = 2$. One layer of checkerboard morphology (+[1]) forms near the lower patterned surface, and about 1.5 bilayers of parallel lamellae (≡) form near the upper homogeneous surface strongly preferring A segments. Refer to Figure 3 for more explanations.

$|||_s$ morphology throughout the entire film; an upper homogeneous surface with relatively strong preference for one of the two blocks would lead to ≡ near the upper surface. For example, the $|||_s$−≡ morphology for the case

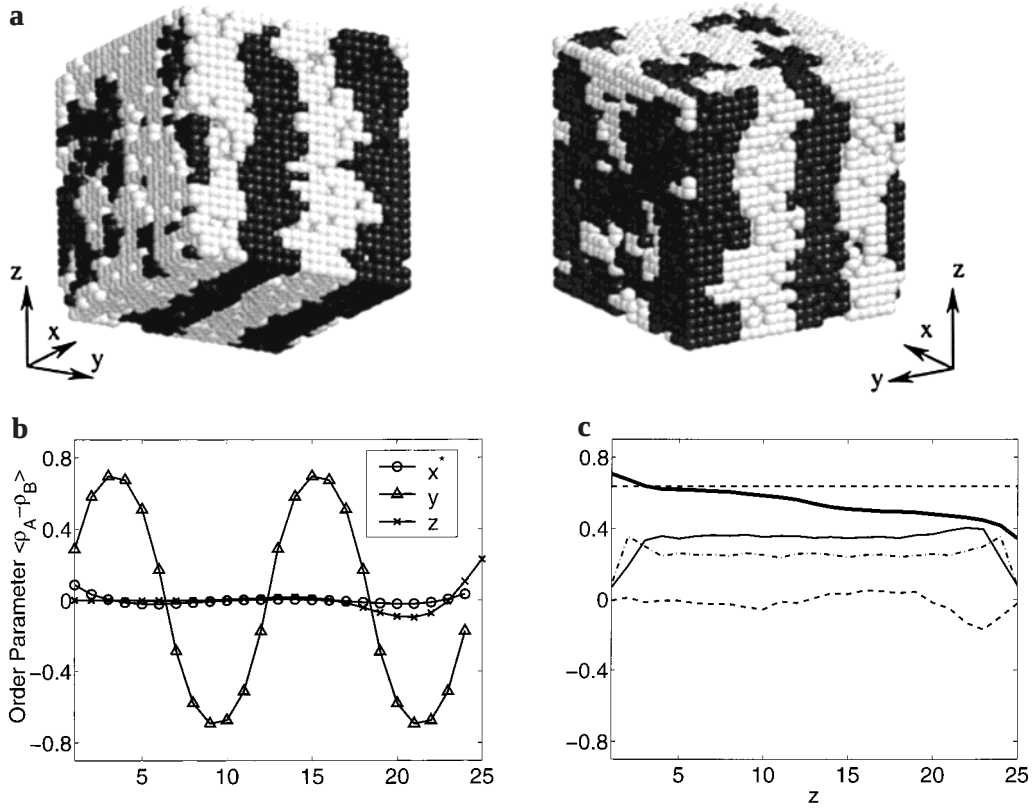

Figure 13. $|||_s$ morphology between patterned-preferential surfaces with $L_s/L_0 = 1$, $D/L_0 = 2$, and $\alpha_H = 0.5$. Perpendicular lamellae complying with the lower surface pattern ($|||_s$) form throughout the entire film. Because of the weak preference of the upper homogeneous surface for A segments, there is some undulation of the A−B interfaces in the perpendicular lamellae. Refer to Figure 3 for more explanations.

$\alpha_H = 1$ and D/L_0=2 is similar to that shown in Figure 10.

In experiments it is difficult to realize a truly neutral surface. In the case of an upper homogeneous and weakly preferential surface (where the $|||_s$ morphology can still form throughout the entire film), the weak preference of the surface may cause some undulation of the A−B interfaces in perpendicular lamellae.[13,17] The preferred segments tend to occupy more surface area near the upper surface; this would lower the surface−block interfacial energy and thus stabilize the perpendicular lamellae. Such morphology for the case $\alpha_H = 0.5$ and $D/L_0 = 2$ is shown in Figure 13. Compared to the $|||_s$ morphology between patterned-neutral surfaces shown in Figure 3, we can see the undulation clearly from the order parameter profile along the z direction, $\langle\rho_A(z) - \rho_B(z)\rangle$, near the upper surface. Furthermore, the slight decrease of the amplitude of the unaligned order parameter profile along the y direction (estimated from the extreme values of $\langle\rho_A(y) - \rho_B(y)\rangle$), i.e., from 0.75 (in the case $\alpha_H = 0$) to 0.69 (in the case $\alpha_H = 0.5$), also reflects the undulation of the A−B interfaces. Similar results are obtained for all other cases where the $|||_s$ morphology forms throughout the entire film between a lower stripe-patterned and an upper weakly preferential surface. Such an undulation could have adverse effects for nanolithography.[13]

4. Summary

We have performed Monte Carlo simulations in an expanded grand-canonical ensemble to study the morphology of symmetric diblock copolymer thin films confined between two hard, flat and parallel surfaces. The upper surface is either neutral or preferential to one of the two blocks, and the lower surface is stripe-patterned.

Two conditions are essential for obtaining macroscopically ordered (over micrometers) perpendicular lamellae in the confined thin films (with film thickness no less than the bulk lamellar period L_0): a stripe-patterned substrate with pattern period L_s comparable to L_0, which directs the ordering of perpendicular lamellae over a macroscopic scale, and a neutral or weakly preferential hard surface on the top of the confined films, which stabilizes the perpendicular lamellae. When the perpendicular lamellae complying with the lower surface pattern form throughout the entire film, undulations of the A−B interfaces in the perpendicular lamellae are observed if the upper surface is not truly neutral, which is often the case in experiments. Such an undulation could have adverse effects for nanolithography.

If the surface pattern period differs from the bulk lamellar period by a small amount, e.g. $L_s/L_0 = {}^2/_3$ or 1.5, we observe some mixed morphology of perpendicular lamellae complying with the surface pattern near the lower patterned surface and perpendicular lamellae of period L_0 near the upper neutral surface. In addition, the height of the lower perpendicular lamellae is almost constant, regardless of surface separation; this results from a reduction of the elastic energy (conformational entropy) cost associated with changing the lamellar period from L_0. Note, however, that only a narrow range of L_s/L_0 exists over which the lamellae near the surface can be stretched or compressed to comply with the lower surface pattern. If the surface pattern period is too large,

e.g. $L_s/L_0 = 2$, chains near the patterned surface change their orientation from parallel to perpendicular to the surface. This results in one layer of checkerboard near the lower surface. On the other hand, if the surface pattern period is too small, e.g. $L_s/L_0 = {}^1/_3$, the patterned surface acts like a homogeneous surface repelling (in this work) the whole chain, and diblock copolymers ignore the surface pattern. Perpendicular lamellae of period L_0 are therefore developed throughout the entire film at lesser cost of increasing surface−block interfacial energy. Note that it would be difficult to achieve macroscopic ordering of the perpendicular lamellae in these systems.

When the upper homogeneous surface is strongly preferential to one of the two blocks, parallel lamellae form near the upper surface. If the period of the lower surface pattern is close to the bulk lamellar period, e.g. $L_s/L_0 = 1$ or ${}^2/_3$, perpendicular lamellae complying with the surface pattern form near the lower surface. If the surface pattern period is large, e.g. $L_s/L_0 = 1.5$ or 2, chains near the surface change their orientation from parallel to perpendicular to the surface, and one layer of checkerboard is observed near the lower surface. On the other hand, if the surface pattern period is too small, e.g. $L_s/L_0 = {}^1/_3$, the patterned surface acts like a homogeneous surface repelling (in this work) the whole chain, and diblock copolymers ignore the surface pattern. In this case, parallel lamellae develop throughout the entire film at the lesser cost of increasing surface−block interfacial energy.

Acknowledgment. Financial support for this work was provided by the Semiconductor Research Corporation through Contract No. 99-LP-452 and by NSF Grants CTS-9703207 and CTS-9901430.

References and Notes

(1) Kellogg, G. J.; Walton, D. G.; Mayes, A. M.; Lambooy, P.; Russell, T. P.; Gallagher, P. D.; Satija, S. K. *Phys. Rev. Lett.* **1996**, *76*, 2503.
(2) Koneripalli, N.; Levicky, R.; Bates, F. S.; Ankner, J.; Kaiser, H.; Satija, S. K. *Langmuir* **1996**, *12*, 6681.
(3) Huang, E.; Russell, T. P.; Harrison, C.; Chaikin, P. M.; Register, R. A.; Hawker, C. J.; Mays, J. *Macromolecules* **1998**, *31*, 7641.
(4) Rockford, L.; Liu, Y.; Mansky, P.; Russell, T. P.; Yoon, M.; Mochrie, S. G. J. *Phys. Rev. Lett.* **1999**, *82*, 2602.
(5) Halperin, A.; Sommer, J. U.; Daoud, M. *Europhys. Lett.* **1995**, *29*, 297.
(6) Chen, H.; Chakrabarti, A. *J. Chem. Phys.* **1998**, *108*, 6897.
(7) Chakrabarti, A.; Chen, H. *J. Polym. Sci., Part B: Polym. Phys.* **1998**, *36*, 3127.
(8) Petera, D.; Muthukumar, M. *J. Chem. Phys.* **1997**, *107*, 9640.
(9) Petera, D.; Muthukumar, M. *J. Chem. Phys.* **1998**, *109*, 5101.
(10) Pereira, G. G.; Williams, D. R. M. *Phys. Rev. Lett.* **1998**, *80*, 2849.
(11) Pereira, G. G.; Williams, D. R. M. *Macromolecules* **1998**, *31*, 5904.
(12) Pereira, G. G.; Williams, D. R. M. *Macromolecules* **1999**, *32*, 758.
(13) Wang, Q.; Nath, S. K.; Graham, M. D.; Nealey, P. F.; de Pablo, J. J. *J. Chem. Phys.*, in press.
(14) Wang, Q.; Yan, Q.; Nealey, P. F.; de Pablo, J. J. *J. Chem. Phys.* **2000**, *112*, 450.
(15) Escobedo, F. A.; de Pablo, J. J. *J. Chem. Phys.* **1996**, *105*, 4391.
(16) Wang, Q.; Yan, Q.; et al. Manuscript in preparation.
(17) G. Pereira, G.; D. R. Williams, M. *Langmuir* 1999, *15* 2125.

MA991293N